Fluorescence enhancement induced by quadratic electric-field effects on dynamics of singlet exciton in poly(3-hexylthiophene) dispersed in poly(methyl methacrylate)

Fluorescence enhancement induced by quadratic electric-field effects on dynamics of singlet exciton in poly(3-hexylthiophene) dispersed in poly(methyl methacrylate)

Toshifumi Iimori,[a] Kamlesh Awasthi,[b] Chin-Shiun Chiou,[b] Eric Wei-Guang Diau,[b,c] Nobuhiro Ohta*[,b,c]

[a]Department of Applied Chemistry, Muroran Institute of Technology, Mizumoto-cho, Muroran 050-8585, Japan.

[b]Department of Applied Chemistry and Institute of Molecular Science, National Chiao Tung University, 1001, Ta-Hsueh Road, Hsinchu 30010, Taiwan.

[c]Center for Emergent Functional Matter Science, National Chiao Tung University, 1001 Ta-Hsueh Rd., Hsinchu 30010, Taiwan.

ABSTRACT

The dynamics of the exciton generated by photoexcitation of regioregular poly(3-hexylthiophene) (P3HT) polymer dispersed into a poly(methyl methacrylate) (PMMA) matrix has been examined by using electro-photoluminescence (E-PL) spectroscopy, where electric field effects on photoluminescence (PL) spectra have been measured. The quadratic electric-field effect have been investigated by using the modulation technique, with which the field-induced change in PL intensity synchronized at the second harmonic of a modulation frequency of the applied electric fields was monitored. Absorption and PL spectra are indicative of the formation both of the ordered crystalline aggregates and of the amorphous regions of P3HT polymer chains. Although previous studies of the electric field effects on π-conjugated polymers showed, in general, that the PL intensity was decreased by electric fields, we report that the PL intensity of P3HT increases and the PL lifetime becomes longer, as the quadratic electric-field effect. The magnitude of the change in PL intensity was quantitatively explained in terms of the field-induced decrease in the nonradiative decay rate constants of exciton. We conjecture that a delayed PL which originates from the recombination of the charge carriers is enhanced in the presence of electric fields. It is also implied that the rate constant of the downhill relaxation process of the exciton, which originates from the relaxation in distributed energy levels due to inherent energetic disorder in P3HT aggregates, becomes smaller in the presence of electric fields. The radiative decay rate constant and PL quantum yield of P3HT dissolved in solution, which are evaluated from the molar extinction coefficient and the PL lifetime, are compared with the ones of P3HT dispersed in a PMMA matrix.

1. Introduction

Conjugated polymers are attracting the highest interest among organic materials because they find applications in inexpensive, flexible, and light-weight materials for electronics and optoelectronics devices.[1-9] While alkyl-substituted polythiophenes are known to show excellent performance as hole transport materials, regio-regular poly(3-hexylthiophene-2,5-diyl) (rr-P3HT) is of primary importance among alkyl-substituted polythiophenes.[10,11]

The photophysics of rr-P3HT has indeed attracted much interest so far and has been studied by using a variety of optical probe techniques.[12-30] Despite numerous studies, the photophysics of elementary excitations in rr-P3HT is complicated and further studies are needed for its fully understanding. The complexity that is specific to rr-P3HT film is due to the presence both of crystalline domains having the coupling among the thiophene units belonging to different polymer chains and of the amorphous portion having lesser degree of the ordering of the polymer chains.

The generation process and the relaxation pathway of the elementary excitd species such as excitons may be influenced by the perturbation of external electric fields. The investigation of such the response of excitons to external electric fields provides us with rich information on the mechanism which is responsible for the photophysics of π-conjugated polymers.[17,18,22,24,28,31-44] Both for the pristine film and for the aggregates of rr-P3HT dispersed in inert matrices, the observations of the photoluminescence (PL) quenching induced by electric fields has been reported by different groups.[18,24,28,41,43,45] As the plausible quenching mechanisms of the singlet exciton, dissociation of the exciton into the electron-hole pair, i.e., the so-called polaron, has typically been argued.[17,35,42,46,47] However, single molecule spectroscopy regarding the electric field effects on the PL intensity of P3HT showed that the electric field was rather inhomogeneous, and single molecules which show PL increase and decrease coexist in a sample.[17] For a derivative of poly(*p*-

phenylene), both the increase and the decrease in PL intensity were similarly observed in the presence of external electric fields, respectively.[36] The mechanism to explain these opposite field effects on the PL intensity is not understood clearly. The current-induced quenching of PL was also observed,[48,49] and then we have to pay attention to the insulation of the P3HT film to investigate intrinsic electric field effects. In addition, PL was monitored at a certain fixed wavelength in the previous studies, but measurements of the electric field effects on the whole PL spectra are of essential importance for the elucidation of the mechanism of the electric field effects on excitation dynamics. In the previous studies, further, electric field effects were measured by monitoring the field-induced change in PL intensity by applying direct current (DC) fields, but experiments using modulation spectroscopy technique are more suitable for the precise determination of the electric field effects on the PL.

Here we report the measurements of the quadratic response of the PL of P3HT to electric fields by using the modulation spectroscopy of the PL spectra, which is called electrophotoluminescence (E-PL) spectroscopy. The mechanism of the electric field effects on PL is also studied by measuring the field-induced change in PL decay profile of P3HT. The quadratic field effect on absorption spectra of P3HT, i.e., electroabsorption (E-A) spectra have been also measured. We used thin films of rr-P3HT dispersed in an insulating PMMA matrix to prevent the injection of charge carriers to P3HT from electrodes. Based on the results, electronic structure and dynamics of P3HT following photoexcitation in the absence and presence of external electric field have been discussed.

2. Experimental Methods

A fluorine-doped tin oxide-coated glass (FTO) substrate (Sinonar) was etched by using zinc powder and HCL solution (4N), and washed with detergent, water/acetone/isopropanol mixture, deionized water, and then cleaned with an ultraviolet–ozone cleaner. Poly(methyl methacrylate) (PMMA) (Aldrich, averaged MW=120 000) was purified by precipitation with a mixture of benzene and methanol and by extraction with hot methanol.

A solution was prepared by dissolving rr-P3HT (Mn 15000–45000, Rieke metals) of 0.67 mg and PMMA of 0.04 g to benzene of 1 mL. The corresponding concentration of P3HT was 1 mol% with respect to the amount of substance (i.e., mol) of the monomer units of PMMA. We prepared a thin film of P3HT dispersed in PMMA by using a spin coating technique with the solution of the mixture of P3HT and PMMA. A semitransparent silver film was prepared onto the P3HT film by using a vacuum deposition technique. The silver film and the FTO substrate were used as electrodes to apply external electric fields (Fig. 1). The thickness of the P3HT dispersed PMMA film was measured with a surface roughness meter (Veeco, Dektak 150). In this work, the thickness was ca. 0.6 μm. In PL measurements in solution, P3HT was dissolved in chlorobenzene with the concentration of 1×10^{-6}M.

All the measurements were carried out at room temperature. In electroabsorption (E-A) measurements, we used a spectrometer (EMV-100, JASCO), the details of which were reported elsewhere, [50,51] and in ESI.

Electro-photoluminescence (E-PL) spectra, which correspond to the electric-field induced change in photoluminescence (PL) spectra, were measured with a commercial spectrofluorometer (JASCO, FP777) combined with a lock-in amplifier, the details of which are described elsewhere, [52] and in ESI. The PL intensity at zero field and its field-induced change are hereafter represented

by I_{PL} and $\Delta I_{\mathrm{PL}} = I_{\mathrm{PL}}(F \neq 0) - I_{\mathrm{PL}}(F = 0)$, respectively. E-PL spectra represent the plots of ΔI_{PL} as a function of wavelength (wavenumber).

PL decay profiles of solid sample in the absence and presence of electric field were measured by using a home-made system. The description of the instrument has been presented elsewhere [53] and in ESI. Briefly, the measurement of decay profiles is based on a time-correlated single photon counting (TCSPC) technique combined with a femtosecond pulsed laser. A multichannel pulse height analyzer (MCA) was used to obtain PL decay profiles. The field-induced change in decay profiles was obtained by using a square-wave voltage pulse train as modulating electric fields. One cycle of the pulse train is composed of the sequence of positive, zero, negative, and zero voltage pulses. In the results, four decay profiles which correspond to positive, zero, negative, and zero bias could be obtained.

PL decay profiles of P3HT in solution were also measured with a TCSPC system (Fluotime 200, PicoQuant) combined with a picosecond pulsed-diode laser having a pulse-width of ~100 ps (LDH-P-C 440, PicoQuant). The repetition rate and pulse-energy of the laser used for the experiments in solution was 0.5 MHz and 1 nJcm^{-2}, respectively.

3. Theoretical background of E-A and E-PL spectroscopy

The field-induced change in absorbance for molecules can be expressed as a linear combination of the zeroth, first, and second derivatives of the absorption spectra: [54-58]

$$\Delta A(\nu) = (fF)^2 \left[A_\chi A(\nu) + B_\chi \nu \frac{\mathrm{d}(A(\nu)/\nu)}{\mathrm{d}\nu} + C_\chi \nu \frac{\mathrm{d}^2(A(\nu)/\nu)}{\mathrm{d}^2\nu} \right] \qquad (1),$$

where ν is the wavenumber of light, $A(\nu)$ is the absorbance at ν, f is the internal field factor, F (=$|\boldsymbol{F}|$) is the field strength. A_χ, B_χ, and C_χ are the coefficients for the zeroth, first, and second derivatives of $A(\nu)$, respectively, and χ is the angle between the external electric field $\boldsymbol{F}$ and the

polarization direction of the excitation light. We now assume that molecules are isotropically oriented, and immobilized in rigid matrices such as the PMMA film. In the experiments with χ = 54.7°, the coefficients B_χ and C_χ in eq1 are given by

$$B_\chi = \frac{\Delta\bar{\alpha}}{2hc}, \qquad C_\chi = \frac{\Delta\mu^2}{6h^2c^2}. \tag{2}$$

We now define $\Delta\boldsymbol{\alpha}$ as the difference in polarizability tensor ($\Delta\boldsymbol{\alpha} = \boldsymbol{\alpha}_e - \boldsymbol{\alpha}_g$), where $\boldsymbol{\alpha}_e$ and $\boldsymbol{\alpha}_g$ are the polarizabilities of the Franck-Condon excited state and the ground state, respectively. In eq2, $\Delta\bar{\alpha}$ is the trace of $\Delta\boldsymbol{\alpha}$, and $\Delta\mu$ (=$|\Delta\boldsymbol{\mu}|$) is the difference of the electric dipole moments between the excited state and the ground state,

$$\Delta\bar{\alpha} = \frac{1}{3}\mathrm{Tr}(\boldsymbol{\alpha}_e - \boldsymbol{\alpha}_g),\ \Delta\mu = \boldsymbol{\mu}_e - \boldsymbol{\mu}_g \tag{3}$$

Here, $\boldsymbol{\mu}_e$ and $\boldsymbol{\mu}_g$ are the electric dipole moments of the excited state and the ground state, respectively. With these equations, we can calculate $\Delta\bar{\alpha}$ and Δμ from the first and the second derivative coefficients B_χ and C_χ in the EA spectra, respectively.

E-PL spectrum is also given by a combination of the zeroth, first and second derivatives of the PL spectrum. For P3HT, as shown later, the coefficient of the zeroth derivative component is of primal importance in electric field effects on PL, and the contribution of the first and second derivative components to the E-PL spectra is minor. The zeroth derivative component shows the change in PL quantum yield induced by the external field (ΔI_{PL}) relative to the unperturbed PL intensity (I_{PL}). Then, electric field effects on photoexcitation dynamics can be discussed, based on the zeroth derivative component of the E-PL spectrum. The mechanism behind the field-induced change in the PL quantum yield can be clarified by studying the field-induced change in fluorescence decay profiles.

4. Results and discussion

Absorption and E-A spectra

Absorption and E-A spectra of the P3HT dispersed in a PMMA matrix are shown in Fig. 2. The magnitude of the field-induced change in absorption intensity was proportional to the square of the applied field strength, as shown in Fig. 2d, as expected from eq1. We simulated the E-A spectrum with a sum of the zeroth, first, and second derivative line shapes of the absorption band shown in Figs. 2a,b. The simulated spectrum is shown in Fig. 2c.

We observed negligibly small contribution of the zeroth-derivative coefficient $A_\chi = 3\times10^{-5}$ $MV^{-2}cm^2$ to the E-A spectrum, indicating that the transition dipole moment of the absorption band was hardly affected by the application of the external electric field $\boldsymbol{F}$. The values of $\Delta\bar{\alpha}$ and $\Delta\mu$ were determined using eq. 2, and we obtained $\Delta\bar{\alpha} = 27$ Å^3 and $\Delta\mu = 1.9$ D, where it is assumed that the internal field factor f is equal to unity.

Similar E-A experiments for a pristine P3HT have been reported by several groups.[15,38,39,44] The principal feature in the E-A spectrum appearing in the range from 15000 to 19000 cm^{-1} was assigned to the Stark shift of the low-lying ^1B_u exciton state. Both the absorption spectra and the E-A spectra for the P3HT in PMMA show very similar features to those for a pristine P3HT film. These results indicate that the structure of P3HT in PMMA is also similar to that in a pristine P3HT film. Actually, for a pristine P3HT film, there exist both the ordered crystalline aggregates and amorphous of P3HT chains in the film.[23] Their absorption spectra are different from each other, and the structured bands appearing at the lower energy below 19000 cm^{-1} are mainly ascribed to the crystalline aggregates of P3HT.[23] The absorption band of the amorphous is broad and shows a maximum intensity above 20000 cm^{-1}. There is the discrepancy between the simulated curve and the observed result in the E-A spectrum in the region above 19000 cm^{-1}. A similar discrepancy was reported in the previous E-A studies of the pristine P3HT film. The discrepancy might be

ascribed to the difference in the molecular parameters and the absorption spectra between the ordered aggregates and amorphous, or to the state mixing with the optically-forbidden $^{m}A_{g}$ exciton state induced by the perturbation of electric fields.[15,38,39]

PL and E-PL spectra

Photoluminescence (PL) spectrum is shown in Fig. 3a. We can decompose the PL spectrum to two bands which show PL maxima at 1.42×10^4 cm^{-1} (704 nm) and 1.55×10^4 cm^{-1} (645 nm). Hereafter, these bands are called G1 and G2 bands, respectively.

E-PL spectrum observed at the second harmonic of the modulation frequency is shown in Fig. 3b. As in the case of E-A spectra, E-PL spectra are usually given by a combination of the zeroth, first and second derivatives of the PL spectrum. Actually, the shape of the observed E-PL spectra is similar to that of the corresponding PL spectrum with a positive signal, indicating that the PL quantum yield increases in the presence of electric field. The E-PL spectra were tried to simulate by using a combination of the zeroth, first and second derivatives of the G1 and G2 bands in the PL spectrum. However, the first and second derivative components were minor in the observed E-PL spectra, and only the zeroth derivative component was important to reproduce the observed E-PL spectra. At excitation wavelength of 450 nm, ΔA of P3HT was so small that we could measure the exact magnitude of the field-induced change in PL spectra. Since the zeroth derivative component gives information regarding the field-induced change in emission quantum yield,[52,59] electric field effects on photoexcitation dynamics can be understood from the zeroth derivative component in the E-PL spectrum.

The magnitude of $\Delta I_{PL}/I_{PL}$ was proportional to the square of the applied field strength, as shown in Fig. 3c. This result shows that the enhancement of the PL quantum yield comes from the quadratic field effect. The magnitude of the field-induced increase in fluorescence quantum yield

could be determined to be 7.4 % and 9.6 % for the G1 and G2 bands, respectively, in the presence of electric field of 0.3 MVcm^{-1}. Then, the field-induced change in PL intensity can be given as follows: $\Delta I_{\mathrm{PL}}/I_{\mathrm{PL}} = 8.2 \times 10^{-1} \times F^2$ for the G1 band, and $\Delta I_{\mathrm{PL}}/I_{\mathrm{PL}} = 1.1 \times F^2$ for the G2 band, where F is the electric field strength in the units of MV cm^{-1}.

Electric field effect on PL of P3HT dispersed in PMMA is different from that for the pristine P3HT film sandwiched between mesoporous TiO_2 and PMMA films (mp-TiO_2/P3HT/PMMA) or between Sb_2S_3 and PMMA films. For example, the values of $\Delta I_{\mathrm{PL}}/I_{\mathrm{PL}}$ for mp-TiO_2/P3HT/PMMA were 0.040 and 0.024 for the G1 and G2 bands, respectively, with a field strength of 0.3 MVcm^{-1}. These values are smaller than the above-mentioned values for P3HT dispersed in a PMMA matrix, indicating that the field-induced PL quenching is more effective for P3HT dispersed in PMMA than that for P3HT solid film.

Fluorescence quantum yield and its field effect

Absorption and PL spectra of P3HT show very different features in solution from those in solid film.[12,23] In this work, we reconfirmed the expected features in solution. As shown in Fig. 4, the absorption spectrum of P3HT in chlorobenzene shows a maximum at 2.22×10^4 cm^{-1} (450 nm) with a nearly single band. The PL spectrum in solution shows a blue shift in comparison with that in the film, even when P3HT is distributed in a PMMA matrix (see Fig. 4). Note that the PL intensity maximum of P3HT is at 1.71×10^4 cm^{-1} (~586 nm) in solution.

The radiative decay rate constant (k_r) in chlorobenzene solution can be calculated by using the following equation,[60]

$$k_r = 2.88 \times 10^{-9} n^2 \frac{g_l}{g_u} \frac{\int I_{PL}(\nu) d\nu}{\int \nu^{-3} I_{PL}(\nu) d\nu} \int \varepsilon(\nu)\, d\ln\nu \qquad (4)$$

where n is the refractive index of the solvent, g_l and g_l are the multiplicities of the ground and the excited states, ν is the wavenumber of light, $I_{PL}(\nu)$ is the intensity of PL at ν, $\varepsilon(\nu)$ is the molar extinction coefficient at ν. Note that both g_l and g_l are equal to 1 in the present study, because our concern is the fluorescence (PL) of P3HT. The calculated radiative decay rate constant k_r of P3HT in chlorobenzene is estimated to be 6.1 x 10^8 s^{-1}, which is very similar to the value reported by Theander et al. for P3HT dissolved in chloroform. i.e., 5.6 x 10^8 s^{-1}.[30] Fluorescence decay of P3HT in chlorobenzene shows a nearly single exponential decay with a lifetime of 560 ps, as shown in Fig. 4, in agreement with the value reported by Cook et al. PL quantum yield (Φ_F) of P3HT in chlorobenzene can be evaluated with PL lifetime (τ) and k_r by the following equation: $\Phi_F = k_r \times \tau$. Then, the magnitude of Φ_F of P3HT in chlorobenzene is determined to be 0.34, which is also good agreement with the one reported by Cook et al., i.e., 0.33 ± 0.007.[12]

It is also possible to obtain the value of k_r from the Φ_F and the PL lifetime. By using $\Phi_F = 0.33$ that was reported by Cook et al. and the PL lifetime $\tau = 560$ ps that was observed in this work, we obtain $k_r = 5.9 \times 10^8$ s^{-1}. This result is very close to that estimated from the absorption coefficient with eq4.

The PL of P3HT dispersed in a PMMA matrix shows a multiexponential decay even without application of electric field, as shown in Figs. 5-7, and the decay profiles were simulated by assuming a tri-exponential decay function of the form of $\sum_{i=1}^{3} A_i \exp\left(-\frac{t}{\tau_i}\right)$. The preexponential factor and the lifetime of each components obtained from the simulation are given in Table 1. The average lifetime (τ_{ave}) which is defined by $\sum_{i=1}^{3} A_i\tau_i / \sum_{i=1}^{3} A_i$ is estimated to be 62 ps for G1 and 64 ps for G2. By using these average lifetimes and by assuming the same k_r for PH3T dispersed in PMMA as that in solution, the magnitude of Φ_F is estimated to be 0.038 for G1 and 0.039 for G2. These values are also comparable to the previously reported value of $\Phi = 0.02$ for a pristine P3HT

film, which was determined from the comparison of the PL spectrum to that for a standard solution of the fluorescence quantum yield.[12]

It is important to note the similar characteristics of the excited state kinetics and similar features of the absorption and PL spectra between the P3HT dispersed in a PMMA matrix and the pristine P3HT film. For the P3HT dispersed in PMMA at a low concentration of 1 mol%, we may expect characteristics similar to those for the solution of P3HT. However, the characteristics are dissimilar to those in solution, and we observed the characteristics rather similar to the P3HT solid film. PL lifetimes of a pristine P3HT film were measured in our previous work, and similar lifetimes were obtained. For example, the components having the lifetime of ca. 40 ps and 200 ps observed for a pristine P3HT film are in good agreement with the components with τ_1 and τ_2 in Table 1. These results suggest that isolated polymer chains do not exist in a PMMA matrix, but polymer chains of P3HT are segregated from PMMA matrix to form aggregations. Thiessen et al. studied the effect of polymer matrices on the structure of P3HT using single molecule fluorescence spectroscopy technique.[26] They visualized the domains of the aggregated P3HT in PMMA matrix in fluorescence micrographs. Moreover, the PL spectra of P3HT in PMMA resembles that in pristine film of P3HT, and there is a striking difference between the present results and those observed in solution (toluene) and in a Zeonex polymer matrix. These results also suggest the formation of the aggregates of P3HT in PMMA due to the phase separation. It is likely that both the aggregates of P3HT formed in a PMMA matrix and the P3HT solid film are composed of the mixture of crystalline domains with lamellar ordering and amorphous phase.[11,61,62]

Change in PL decay profile induced by electric fields

In the steady-state measurements of E-PL spectra, we observed the enhancement of the PL quantum yield due to the quadratic electric field effects (Fig. 3). The mechanisms in the electric-

field effects on PL intensity can be investigated by measuring the change in PL decay profiles induced by electric fields, since the change in the PL quantum yield can be caused by the electric field-induced change in population and/or decay kinetics at the emitting state. The emitting state is not directly produced upon photoexcitation, but produced after the relaxation from the Franck-Condon photoexcited state.[44] If the rate constants of any decay processes from the Franck-Condon photoexcited state are affected by electric fields, the yield of the emitting state should change. The changes in decay rate constants at the emitting state also lead to the change in the quantum yield of PL. The enhancement of the PL quantum yield, as observed in this study, can occur if the sum of the nonradiative decay rate constants of the emitting state is decreased by application of electric fields. The increase in k_r may also result in the increase of the PL quantum yield.

We measured the PL decay profiles in the presence and absence of the electric field of 0.3 MV cm^{-1}. Hereafter, the decay profiles measured in the presence of positive, zero, negative, and zero voltages are denoted by Channel 1 (CH1), Channel 2 (CH2), Channel 3 (CH3), and Channel 4 (CH4), respectively. The description of the measurements of the decay profiles is given in ESI. In the steady-state E-PL measurements, we measured the quadratic electric field effects on the PL intensity. We can investigate the changes in the decay profiles which originate from the quadratic electric field effects, as stated in the following. The decay profile in the presence of the electric field of 0.3 $MVcm^{-1}$ can be obtained by the sum of CH1 and CH3, and the decay profile in the absence of the electric field is obtained as the sum of CH2 and CH4. Note that CH2 and CH4 give essentially the same decay profile, as shown in ESI (Fig. S2). We hereafter use $I_{ON}(t)$ and $I_{OFF}(t)$ to represent the decay profiles obtained by CH1 + CH3, and CH2 + CH4 for the F = 0.3 MV cm^{-1} and zero, respectively. CH1 and CH3 show the decay profiles observed in the presence of + 0.3 and – 0.3 $MVcm^{-1}$, respectively. It is expected that the linear electric field effect on PL shows a

drastic difference in field-induced change in decay profile, when the direction of the applied electric field is inverted. This is true in P3HT solid film sandwiched between TiO_2 and PMMA films or sandwiched between Sb_2S_3 and PMMA films.[44] In P3HT dispersed in a PMMA matrix, however, CH1 and CH3 show very similar electric field effect on PL decay profile, as shown in Figs. 5 and 6. In P3HT polymer chains dispersed in a PMMA matrix, therefore, the linear electric field effect on PL is very small, if any, and the quadratic field effect is known to be dominant.

The decay profiles of $I_{ON}(t)$ and $I_{OFF}(t)$ are shown in Fig. 7. The time profile of the difference $(I_{ON}(t) - I_{OFF}(t))$ shows positive signal over the range of the timescale measured in this work (Figs. 7 c and g). This result agrees with the results of the steady-state E-PL measurements, which indicates the enhancement of the PL intensity in the presence of external electric fields. The intensity of $(I_{ON}(t) - I_{OFF}(t))$ integrated in the whole time range is about 9% of the integrated intensity of $I_{OFF}(t))$ both in G1 and G2, which is fair agreement with the steady-state experiment. The time profiles of the ratio $(I_{ON}(t)/I_{OFF}(t))$ is nearly one at $t = 0$, indicating that the pre-exponential factors of the each decay components are little affected by the electric field for both G1 and G2. In addition, in the time profiles of the ratio, the value increases with time after the photoexcitation. This result qualitatively indicates the elongation of the decay lifetime in the presence of the electric field.

The above qualitative argument is quantitatively confirmed through the analysis of the field-induced change in PL decay profiles. The lifetimes and pre-exponential factors for $I_{ON}(t)$ and $I_{OFF}(t)$ were determined by assuming a tri-exponential decay function. It was possible to precisely determine the subtle changes in lifetimes and pre-exponential factors induced by the electric fields by simultaneously reproducing the difference and the ratio between $I_{ON}(t)$ and $I_{OFF}(t)$ in the decay analysis. In Table 1, the pre-exponential factors and lifetimes of the three exponential components

in the tri-exponential decay function are summarized. The average lifetimes τ_{ave} become longer in the presence of electric fields. The field-induced changes in the pre-exponential factors are minor, showing that the initial population of the emitting state of P3HT is little affected by electric fields.

As the mechanism of the enhancement of the PL quantum yield observed in the E-PL spectra, we can consider that the sum of nonradiative decay rate constants of the emitting state becomes smaller in the presence of electric fields. The change in the PL quantum yield ($\Delta\Phi(F)$) induced by $\boldsymbol{F}$ can be related to the change in the sum of the nonradiative decay rate constants ($\Delta k_{nr}(F)$):[55,59] $\Delta\Phi(F) = -\Delta k_{nr}(F) \times \tau$, where τ is the PL lifetime in the absence of $\boldsymbol{F}$. We can examine this mechanism from the data of E-PL spectra and the decay profiles, if we take $\Delta I_{\mathrm{PL}}/I_{\mathrm{PL}}$ as $\Delta\Phi(F)$, τ_{ave} of $I_{\mathrm{OFF}}(t)$ as τ, and the difference between the values of $1/\tau_{\mathrm{ave}}$ for $I_{\mathrm{ON}}(t)$ and $I_{\mathrm{OFF}}(t)$ as $\Delta k_{nr}(F)$, respectively. We then obtain $\Delta k_{nr}(F) = -1.3 \times 10^{9}\ \mathrm{s}^{-1}$ at 0.3 MVcm^{-1} and $\tau = 6.4 \times 10^{-11}\ \mathrm{s}^{-1}$ at the PL wavelength of 640 nm, i.e., for G2. By using these two terms, $\Delta\Phi(F)$ is obtained to be 8.3×10^{-2} in the presence of 0.3 MVcm^{-1}. This value is in good agreement with the $\Delta I_{\mathrm{PL}}/I_{\mathrm{PL}} = 9.6 \times 10^{-2}$ experimentally observed for the G2 band in the E-PL spectrum at 0.3 MV cm^{-1}. Thus, the field-induced enhancement of the PL quantum yield is induced by the change in the sum of the nonradiative rate constants at the PL emitting state. The zeroth derivative component of A_{χ} in the EA spectrum was negligibly small with the order of 10^{-5}, and therefore the contribution of the change in the radiative decay rate constant is known to be negligible.

Mechanism of field-induced PL enhancement

The results on the PL decay profile have demonstrated that (1) the field-induced enhancement of the PL intensity can be ascribed to the elongation of PL lifetime in the presence of electric fields, and (2) the field-induced change in the population of the emitting state is very small.

It has been suggested that the charge carrier is generated from the dissociation of hot (unrelaxed) excitons and this process takes place very promptly.[12,13,44,61,63] This process competes with the generation process of the relaxed singlet exciton. In a pristine P3HT film sandwiched between mp-TiO_2 and PMMA films or between Sb_2S_3 and PMMA films, we hardly observed the change of the preexponential factors induced by quadratic electric field effects, although the change was observed as the result of the first-order electric field effects.[44] In the P3HT film dispersed in PMMA, we obtained the similar results for which the change of the preexponential factors was hardly observed. These results indicate that the dissociation rate of the hot exciton produced directly by photoexcitation does not show the quadratic electric field effect, because the branching ratio between the emitting state and the charge carriers depends on the dissociation rate of the hot exciton.

The assignment of each decay component observed in the range from hundreds of femtosecond to nanosecond timescales which has been proposed to date includes a torsional relaxation toward a planar configuration of thiophene units in P3HT chains with a relaxation time of 13 ps[16] and the diffusion process of the exciton. The diffusion is explained in terms of downhill relaxation due to energy transfer, in which the excitons migrate toward sites with lower energy levels in the density-of-states (DOS) of the energy band of P3HT.[35,62,64,65]In general, the downhill relaxation of singlet excitons occurs with timescales in the range from pico- to nanosecond. The delayed PL which asymptotically decays with a power law and lasts until $t \geq 10$ ns has also been observed which originates from the recombination of charge carriers.[17,20,25,66]

We have observed that the curves of the ratio ($I_{ON}(t)/I_{OFF}(t)$) of the decay profiles become larger as time windows become later (Figs. 7d, h). This behavior may suggest that the relatively slower dynamics of the exciton and/or charge carriers are significantly affected by electric fields. The value of the ratio greater than 1 corresponds to the PL enhancement, and the enhancement factor reaches ≈ 1.4 at 1.0 ns. We conjecture that the delayed PL due to the recombination of the charge carriers is increased by the quadratic electric-field effects. But it is noted that the field-induced change in intensity estimated from the integration of the PL decay profile is almost the same as the one obtained in the steady-state measurement, as already mentioned. This implies that the electric field effect is concerned with the dynamic of P3HT which occurs in the subnanosecond time scale. We can tentatively assign the lifetime component of τ_3 to the delayed PL. The component τ_3 shows a significant increase as the result of the quadratic electric-field effects (see Table 1). It has been reported that the delayed PL showed a decay obeying a power law in the form of $\approx t^{-(1+\mu)}$, where the parameter μ is given by the ratio of the characteristic electron-hole distance for the distribution of their distances, and the distance dependence (denoted by β) of the tunneling probability for the recombination.[20] On this model, the PL decay becomes slower if the electron-hole distance decreases, or the β increases. If any of these changes can be induced by electric fields, the PL enhancement is consequently observed. The value of the ratio around $t = 0$ is close to the unity, indicating the relatively faster dynamics including the conformational planarization and the relaxation of the hot exciton is hardly affected by electric fields.

We can explain the observed result if the downhill relaxation rate becomes slower in the presence of electric fields. The field-induced change in the energy transfer rate might be significant if the distribution of the energy levels within the DOS is sparse. The DOS in the P3HT aggregate is unambiguously not sparse, and the perturbation on the energy transfer rate might be insignificant.

However, we observed the field-induced increase in the PL lifetimes over the timescales in the range from tens to hundreds of picoseconds in the lifetime components of τ_1 and τ_2, and these timescales parallel those for the downhill relaxation, as stated earlier. This fact might imply that the decrease of the energy transfer rate causing the downhill relaxation is induced by electric fields. Actually speaking, however, we cannot give clear interpretation about the mechanism with which energy transfer of P3HT is reduced by application of electric field, and the electric field effect on the delayed fluorescence may be more plausible.

Previous studies on the electric field effects on the PL of π-conjugated polymers have, in general, shown that the PL is quenched by electric fields. However, we have observed the opposite effect, i.e., the field-induced increase of the PL for the P3HT dispersed in PMMA. In our previous work for the pristine P3HT film, the increase of the PL was similarly observed with the quadratic electric field effects.[44] Note that both the increase and quenching of the PL were observed in the presence of electric field when a single-molecule spectroscopy was used without ensemble averaging.[17,36] We have already investigated the first-order electric field effects for the pristine P3HT film sandwiched between mp-TiO_2 and PMMA films or between Sb_2S_3 and PMMA films, and we have reported that both the increase and decrease of the PL intensity were observed depending on the direction of the external electric field.[44] The anisotropy of the field-induced change in PL with respect to the field direction of the applied electric fields can be explained in terms of the synergy effect between internal electric field which exists in the P3HT film and externally applied electric field.[44] Based on this result, it is likely that the variation of the electric field effects observed in single-molecule spectroscopy results from the inhomogeneity in the internal electric fields which may intrinsically exist due to local inhomogeneity of the medium and the structural fluctuation of the polymer chains. The field-induced quenching of the PL reported

so far may be also explained by invoking the quenching induced by the current. In the present work, the P3HT was dispersed at a dilute concentration in the insulating PMMA film, and thus we can neglect the contribution of the current-induced quenching of the PL. The direction of the electric field can also be a factor which determines the increase or the decrease of the PL. The previous studies observing the quenching of PL employed the static DC electric field in the experiments. The PL quenching observed in the previous studies might be induced by the synergy effect between the internal electric field, which may exist by reasons as stated above, and the externally applied electric field. Under this mechanism, we might expect the increase of the PL, when the direction of the external DC electric field is reversed. In the present experiments, we used the modulation technique where the PL signal synchronized with the modulation frequency at the second-harmonic of the applied alternating-current (AC) electric field was detected. Further, linear electric field effect caused by the anisotropic property of the sample can be neglected in P3HT dispersed in PMMA, in contrast with the P3HT films sandwiched between TiO_2 and PMMA or between Sb_2S_3 and PMMA films. Therefore, we have obtained the intrinsic external electric field effects on the PL of P3HT aggregates without the contribution of the internal electric field effects.

5. Conclusion

The dynamics of the excitons in P3HT dispersed in a PMMA film was studied with the E-A and E-PL spectroscopies. In a PMMA matrix, the formation of the crystalline aggregate is indicated for P3HT polymer chains by the similarity of the absorption and PL spectra to those for the pristine P3HT film. The previous studies for the electric field effects on the PL of π-conjugated polymers including P3HT have, in general, reported the quenching of the PL. On contrary to these

previous results, the increase of the PL intensity was observed as the result of the quadratic electric field effects. The field-induced increase of PL intensity is more effective in P3HT dispersed in a PMMA matrix in comparison to the pristine P3HT film. The measurements of the field-induced change in PL decay profiles showed that the increase of the PL intensity is caused by the decrease of the nonradiative decay rate constant, which is mainly ascribed to the increase of the delayed PL due to the recombination of the charge carriers at the emitting state in the presence of electric fields.

Electronic Supplementary Information (ESI) available:

Details of E-A and E-PL spectroscopy and time-resolved E-PL measurements. See DOI: 10.1039/xxxxxxxxxx.

AUTHOR INFORMATION

Corresponding Authors

*E-mail: nohta@nctu.edu.tw (N.O)

The authors declare no competing financial interest.

ACKNOWLEDGMENT

Ministry of Science and Technology (MOST) in Taiwan provided financial support of this research (MOST107-2113-M-009-005, MOST107-3017-F009-003). This work was also financially supported by the Center for Emergent Functional Matter Science of National Chiao

Tung University from The Featured Areas Research Center Program within the framework of the Higher Education Sprout Project by the Ministry of Education (MOE) in Taiwan.

REFERENCES

1 W. Barford, *Electronic and optical properties of conjugated polymers*, Oxford University Press, Oxford, 2005.

2 P. Bujak, I. Kulszewicz-Bajer, M. Zagorska, V. Maurel, I. Wielgus and A. Pron, *Chem. Soc. Rev.,* 2013, **42,** 8895-8999.

3 S. Günes, H. Neugebauer and N. S. Sariciftci, *Chem. Rev.,* 2007, **107**, 1324-1338.

4 T. M. Clarke and J. R. Durrant, *Chem. Rev.,* 2010, **110**, 6736-6767.

5 F. C. Spano and C. Silva, *Annu. Rev. Phys. Chem.,* 2014, **65,** 477-500.

6 O. Ostroverkhova, *Chem. Rev.,* 2016, **116**, 13279-13412.

7 O. Itaru and T. Kazuo, *Adv. Mater.,* 2017, **29,** 1605218.

8 A. Facchetti, *Chem. Mater.,* 2011, **23**, 733-758.

9 L. Ying, F. Huang and G. C. Bazan, *Nature Commun.,* 2017, **8**, 14047.

10 H. Sirringhaus, P. J. Brown, R. H. Friend, M. M. Nielsen, K. Bechgaard, B. M. W. Langeveld-Voss, A. J. H. Spiering, R. A. J. Janssen, E. W. Meijer, P. Herwig and D. M. de Leeuw, *Nature,* 1999, **401**, 685-688.

11 H. Sirringhaus, *Adv. Mater.,* 2005, **17**, 2411-2425.14.

12 S. Cook, A. Furube and R. Katoh, *Energy Environ. Sci.,* 2008, **1**, 294-299.

13 J. Guo, H. Ohkita, H. Benten and S. Ito, *J. Am. Chem. Soc.,* 2009, **131**, 16869-16880.

14 X. M. Jiang, R. Österbacka, O. Korovyanko, C. P. An, B. Horovitz, R. A. J. Janssen and Z. V. Vardeny, *Adv. Funct. Mater.,* 2002, **12**, 587-597.

15 R. Österbacka, C. P. An, X. M. Jiang and Z. V. Vardeny, *Science,* 2000, **287**, 839-842.

16 P. Parkinson, C. Müller, N. Stingelin, M. B. Johnston and L. M. Herz, *J. Phys. Chem. Lett.,* 2010, **1**, 2788-2792.

17 T. Sugimoto, S. Habuchi, K. Ogino and M. Vacha, *J. Phys. Chem. B,* 2009, **113**, 12220-12226.

18 A. K. Thomas, H. A. Brown, B. D. Datko, J. A. Garcia-Galvez and J. K. Grey, *J. Phys. Chem. C,,* 2016, **120**, 23230-23238.

19 N. Banerji, S. Cowan, E. Vauthey and A. J. Heeger, *J. Phys. Chem. C,* 2011, **115**, 9726-9739.

20 F. Paquin, G. Latini, M. Sakowicz, P.-L. Karsenti, L. Wang, D. Beljonne, N. Stingelin and C. Silva, *Phys. Rev. Lett.,* 2011, **106**, 197401.

21 P. J. Brown, D. S. Thomas, A. Köhler, J. S. Wilson, J.-S. Kim, C. M. Ramsdale, H. Sirringhaus and R. H. Friend, *Phys. Rev. B,* 2003, **67**, 064203.

22 P. J. Brown, H. Sirringhaus, M. Harrison, M. Shkunov and R. H. Friend, *Phys. Rev. B,* 2001, **63**, 125204.

23 J. Clark, C. Silva, R. H. Friend and F. C. Spano, *Phys. Rev. Lett.,* 2007, **98**, 206406.

24 K. E. Ziemelis, A. T. Hussain, D. D. C. Bradley, R. H. Friend, J. Rühe and G. Wegner, *Phys. Rev. Lett.,* 1991, **66**, 2231-2234.

25 F. Paquin, J. Rivnay, A. Salleo, N. Stingelin and C. Silva-Acuna, *J. Mater. Chem. C,* 2015, **3**, 10715-10722.

26 A. Thiessen, J. Vogelsang, T. Adachi, F. Steiner, D. Vanden Bout and J. M. Lupton, *Proc. Natl. Acad. Sci*., 2013, **110**, E3550-E3556.

27 B. Ferreira, P. F. da Silva, J. S. Seixas de Melo, J. Pina and A. Maçanita, *J. Phys. Chem. B,* 2012, **116**, 2347-2355.

28 C. Deibel, D. Mack, J. Gorenflot, A. Schöll, S. Krause, F. Reinert, D. Rauh and V. Dyakonov, *Phys. Rev. B*, 2010, **81**, 085202.

29 O. J. Korovyanko, R. Österbacka, X. M. Jiang, Z. V. Vardeny and R. A. J. Janssen, *Phys. Rev. B*, 2001, **64**, 235122.

30 M. Theander, O. Inganäs, W. Mammo, T. Olinga, M. Svensson and M. R. Andersson, *J. Phys. Chem. B*,1999, **103**, 7771-7780.

31 J. Cabanillas-Gonzalez, G. Grancini and G. Lanzani, *Adv. Mater.*, 2011, **23**, 5468-5485.

32 M. S. Mehata, C.-S. Hsu, Y.-P. Lee and N. Ohta, *J. Phys. Chem. B*, 2010, **114**, 6258-6265.

33 P. R. Hania, D. Thomsson and I. G. Scheblykin, *J. Phys. Chem. B*, 2006, **110,** 25895-25900.

34 I. Scheblykin, G. Zoriniants, J. Hofkens, S. De Feyter, M. Van der Auweraer and F. C. De Schryver, *ChemPhysChem*, 2003, **4**, 260-267.

35 I. G. Scheblykin, A. Yartsev, T. Pullerits, V. Gulbinas and V. Sundstrom, *J. Phys. Chem. B,* 2007, **111**, 6303.

36 F. Schindler, J. M. Lupton, J. Müller, J. Feldmann and U. Scherf, *Nature Mater.*, 2006, **5**, 141.

37 T. M. Smith, J. Kim, L. A. Peteanu and J. Wildeman, *J. Phys. Chem. C*, 2007, **111**, 10119-10129.

38 M. Liess, S. Jeglinski, Z. V. Vardeny, M. Ozaki, K. Yoshino, Y. Ding and T. Barton, *Phys. Rev. B*, 1997, **56**, 15712-15724.

39 K. Sakurai, H. Tachibana, N. Shiga, C. Terakura, M. Matsumoto and Y. Tokura, *Phys. Rev. B*, 1997, **56**, 9552-9556.

40 J. D. McNeill, D. B. O'Connor, D. M. Adams, P. F. Barbara and S. B. Kämmer, *J. Phys. Chem. B,* 2001, **105**, 76-82.

41 R. Kersting, U. Lemmer, R. F. Mahrt, K. Leo, H. Kurz, H. Bässler and E. O. Göbel, *Phys. Rev. Lett.*, 1993, **70**, 3820-3823.

42 R. Kersting, U. Lemmer, M. Deussen, H. J. Bakker, R. F. Mahrt, H. Kurz, V. I. Arkhipov, H. Bässler and E. O. Göbel, *Phys. Rev. Lett.*, 1994, **73**, 1440-1443.

43 V. I. Arkhipov, H. Bässler, M. Deussen, E. O. Göbel, R. Kersting, H. Kurz, U. Lemmer and R. F. Mahrt, *Phys. Rev. B*, 1995, **52**, 4932-4940.

44 T. Iimori, K. Awasthi, C.-S. Chiou, E. W.-G. Diau and N. Ohta, *ACS Appl. Energy Mater.*, 2018, **1**, 6136-6151.

45 M. Deussen, M. Scheidler and H. Bässler, *Synthetic Metals*, 1995, **73**, 123-129.

46 W. Graupner, G. Cerullo, G. Lanzani, M. Nisoli, E. J. W. List, G. Leising and S. De Silvestri, *Phys. Rev. Lett.,* 1998, **81**, 3259-3262.

47 V. Gulbinas, Y. Zaushitsyn, V. Sundström, D. Hertel, H. Bässler and A. Yartsev, *Phys. Rev. Lett.*, 2002, **89**, 107401.

48 E. T. Niles, J. D. Roehling, H. Yamagata, A. J. Wise, F. C. Spano, A. J. Moulé and J. K. Grey, *J. Phys. Chem. Lett.,* 2012, **3**, 259-263.

49 A. J. Ferguson, N. Kopidakis, S. E. Shaheen and G. Rumbles, *J. Phys. Chem. C*, 2008, **112**, 9865-9871.

50 H.-C. Chiang, T. Iimori, T. Onodera, H. Oikawa and N. Ohta, *J. Phys. Chem. C*, 2012, **116**, 8230-8235.

51 J. Tayama, T. Iimori and N. Ohta, *J. Chem. Phys.*, 2009, **131**, 244509.

52 N. Ohta, *Bull. Chem. Soc. Jpn.*, 2002, **75**, 1637-1655.

53 M. Tsushima, T. Ushizaka, N. Ohta, *Rev. Sci. Instrum.*, 2004, **75**, 479-485.

54 S. G. Boxer, *J. Phys. Chem. B*, 2009, **113**, 2972-2983.

55 N. Ohta, *Pure Appl. Chem.,* 2013, **85**, 1427-1435.

56 W. Liptay, In *Excited States*; Lim, E. C., Ed.; Academic Press: New York, 1974; Vol. 1, p 129.

57 S. A. Locknar, A. Chowdhury, L. A. Peteanu, *J. Phys. Chem. B,* 2000, **104**, 5816-5824.

58 E. Jalviste, N. Ohta, *J. Photochem. Photobio. C: Photochem. Rev.,* 2007, **8**, 30-46.

59 T. Iimori, R. Ito and N. Ohta, *J. Phys. Chem. A*, 2016, **120**, 5497-5503.

60 S. J. Strickler, and R. A. Berg, *J. Chem. Phys.,* 1962, **37**, 814-822.

61 J. Piris, T. E. Dykstra, A. A. Bakulin, P. H. M. v. Loosdrecht, W. Knulst, M. T. Trinh, J. M. Schins and L. D. A. Siebbeles, *J. Phys. Chem. C*, 2009, **113**, 14500-14506.

62 Y. Tamai, H. Ohkita, H. Benten and S. Ito, *J. Phys. Chem. Lett.*, 2015, **6**, 3417-3428.

63 C. X. Sheng, M. Tong, S. Singh and Z. V. Vardeny, *Phys. Rev. B,* 2007, **75**, 085206.

64 F. Laquai, Y.-S. Park, J.-J. Kim and T. Basché, *Macromol. Rapid Commun.*, 2009, **30**, 1203-1231.

65 I. Hwang and G. D. Scholes, *Chem. Mater.,* 2011, **23**, 610-620.

66 J. A. Labastide, M. Baghgar, I. Dujovne, B. H. Venkatraman, D. C. Ramsdell, D. Venkataraman and M. D. Barnes, *J. Phys. Chem. Lett.*, 2011, **2**, 2089-2093.

Table 1. Lifetime (τ_i) in the unit of ps, and pre-exponential factor (given in parentheses) of each decaying component of PL observed at a field strength of 0.3 MV cm^{-1} measured as $I(t)_{ON}$ = CH1+CH3, and at zero field measured as $I(t)_{OFF}$ = CH2+CH4. The average lifetime (τ_{ave}) and the sum of the pre-exponential factors ($\sum_{i=1}^{3} A_i$) in each decay profile are also shown. The sum of the pre-exponential factors are normalized to be unity for the decay profile at zero field. The PL was monitored at wavelengths λ = 640 and 705 nm, respectively, for the G2 and G1 bands.

λ	F (MV cm^{-1})	τ_1(ps) (A_1)	τ_2(ps) (A_2)	τ_3(ps) (A_3)	τ_{ave}(ps) ($\sum_{i=1}^{3} A_i$)
640 nm	0.3	39.2 (0.754)	130 (0.239)	432 (0.027)	70 ± 4.3 (1.020)
	0	37.8 (0.752)	121 (0.225)	411 (0.023)	64 ± 3.6 (1.000)
705 nm	0.3	37.3 (0.738)	125 (0.246)	438 (0.027)	69 ± 4.2 (1.011)
	0	34.1 (0.732)	111 (0.242)	376 (0.026)	62 ± 3.5 (1.000)

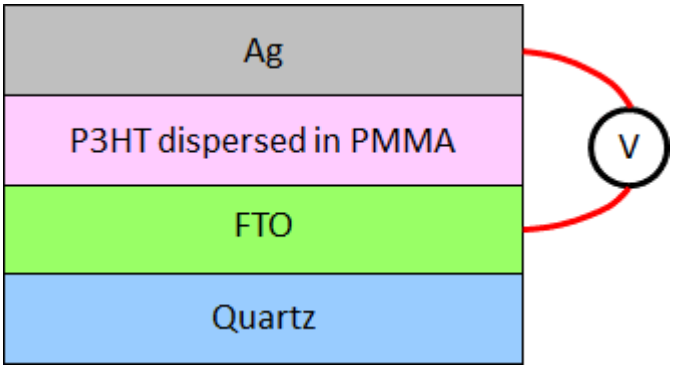

Fig. 1. Layer structure of the device used in the present work. FTO and Ag films were used as electrodes to apply external voltages (V) to the P3HT dispersed in a PMMA matrix.

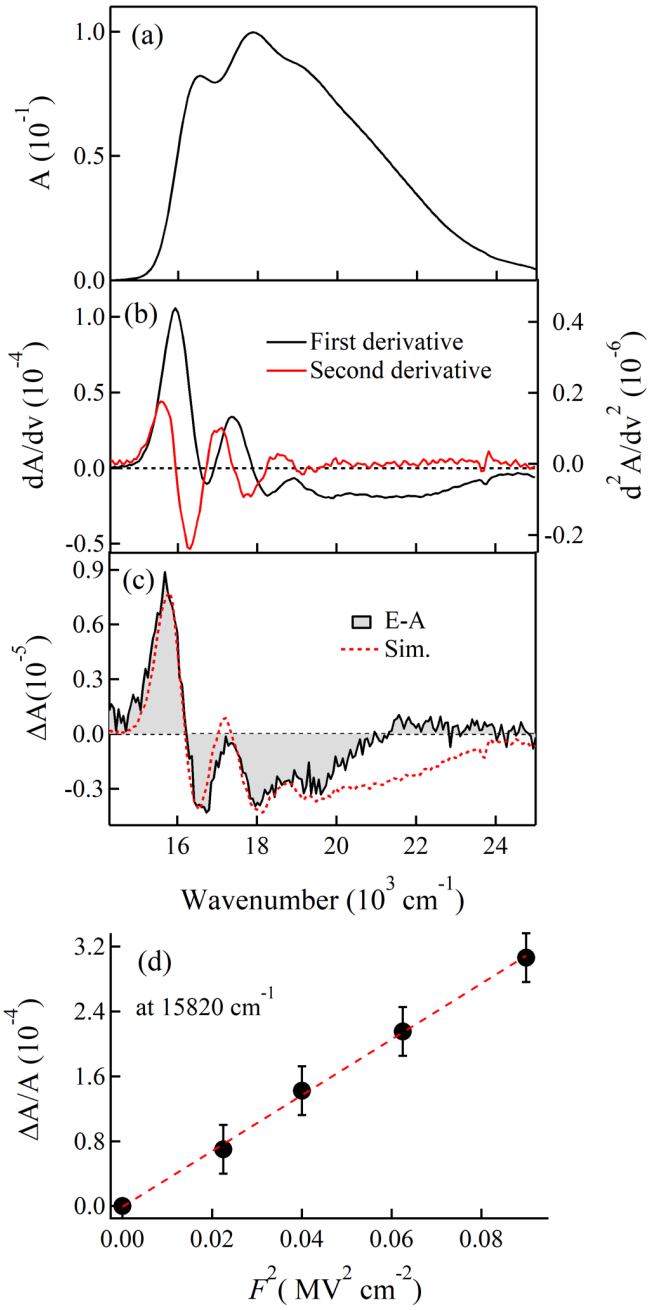

Fig. 2. Absorption spectrum of P3HT dispersed in a PMMA matrix (a), the first and the second derivatives of the absorption spectrum (b), E-A spectrum observed with a field strength of 0.3 $MVcm^{-1}$ (c), and plots of the field-induced change in absorption intensity at 15820 cm^{-1} (d). In (c), the black line shows the observed spectrum, and the red line shows the simulated spectrum.

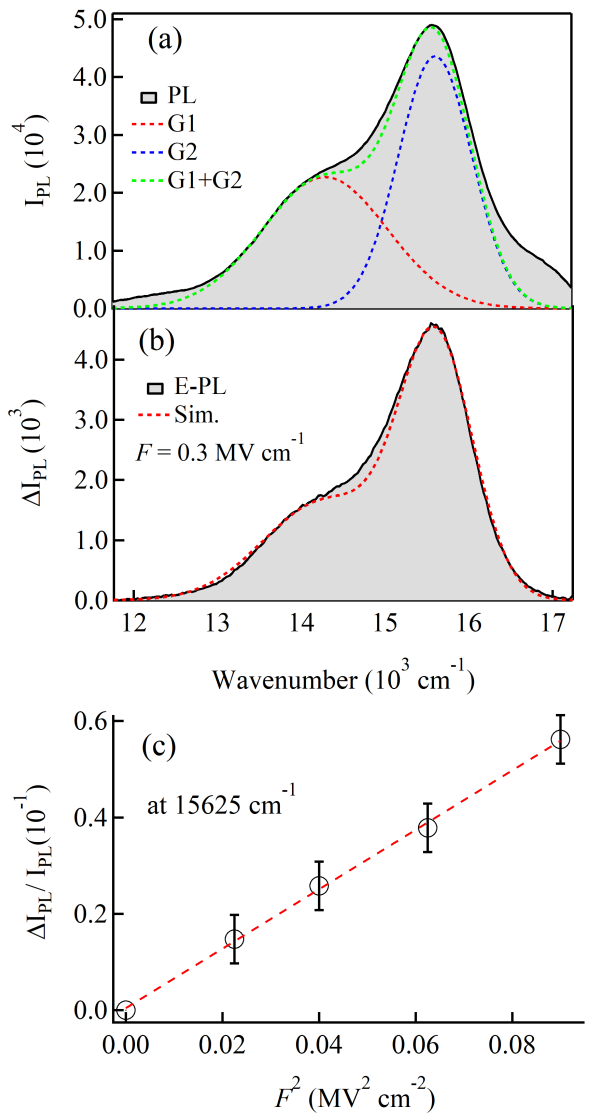

Fig. 3. PL and E-PL spectra with excitation at 450 nm. (a) PL spectrum and the decomposition to the G1 and G2 bands, which were used for the simulation of the E-PL spectrum. (b) E-PL spectrum observed with a field strength of 0.3 MVcm^{-1} (black solid line), and the simulated spectrum (red broken line). (c) Plots of $\Delta I_{PL}/I_{PL}$ as a function of the square of applied field strength. E-PL spectrum was monitored at the second harmonic of the modulation frequency.

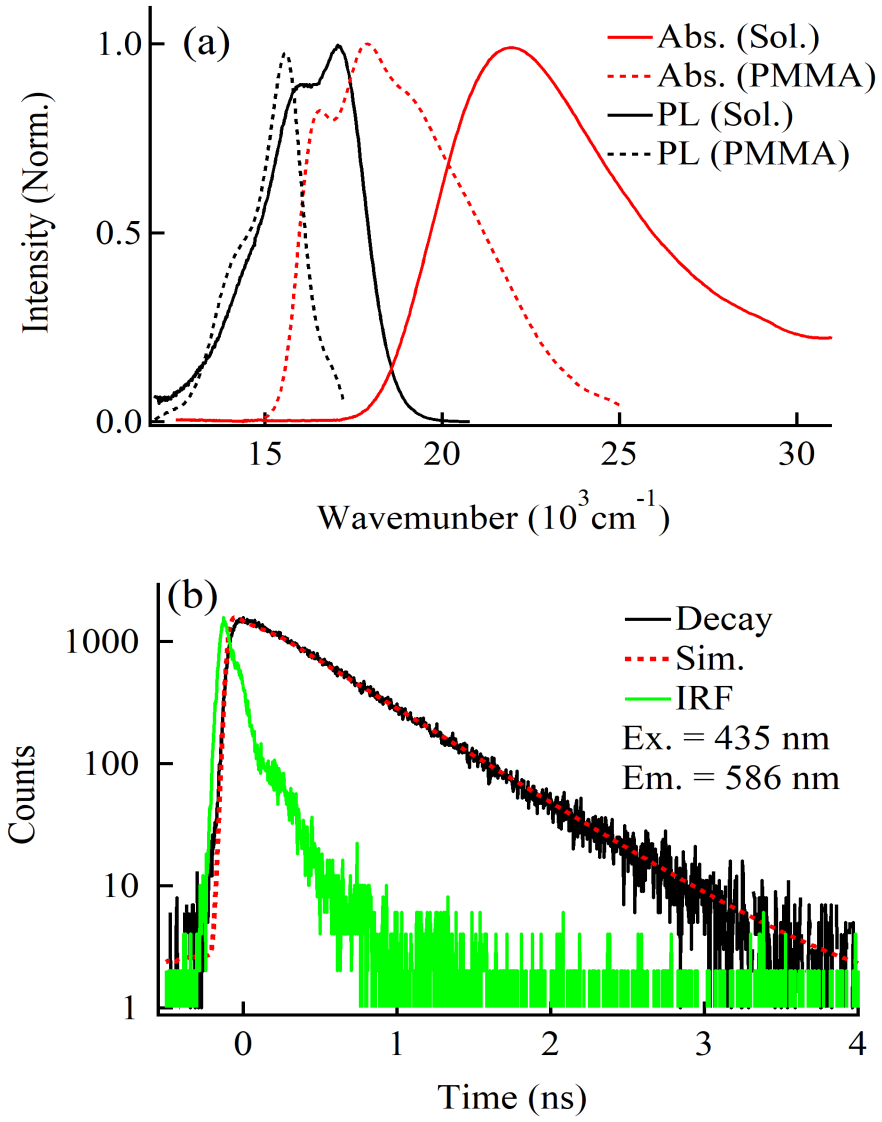

Fig. 4. (a) Absorption spectra (red line) and PL spectra (black line) of P3HT in solution (solid line) and P3HT distributed in a PMMA matrix (broken line). (b) PL decay profile in solution (black line) observed at 586 nm with excitation at 435 nm, the instrumental response function (IRF) (green line), and the decay simulated by assuming a single exponential function (red line). PL spectra in (a) were obtained with excitation at 450 nm.

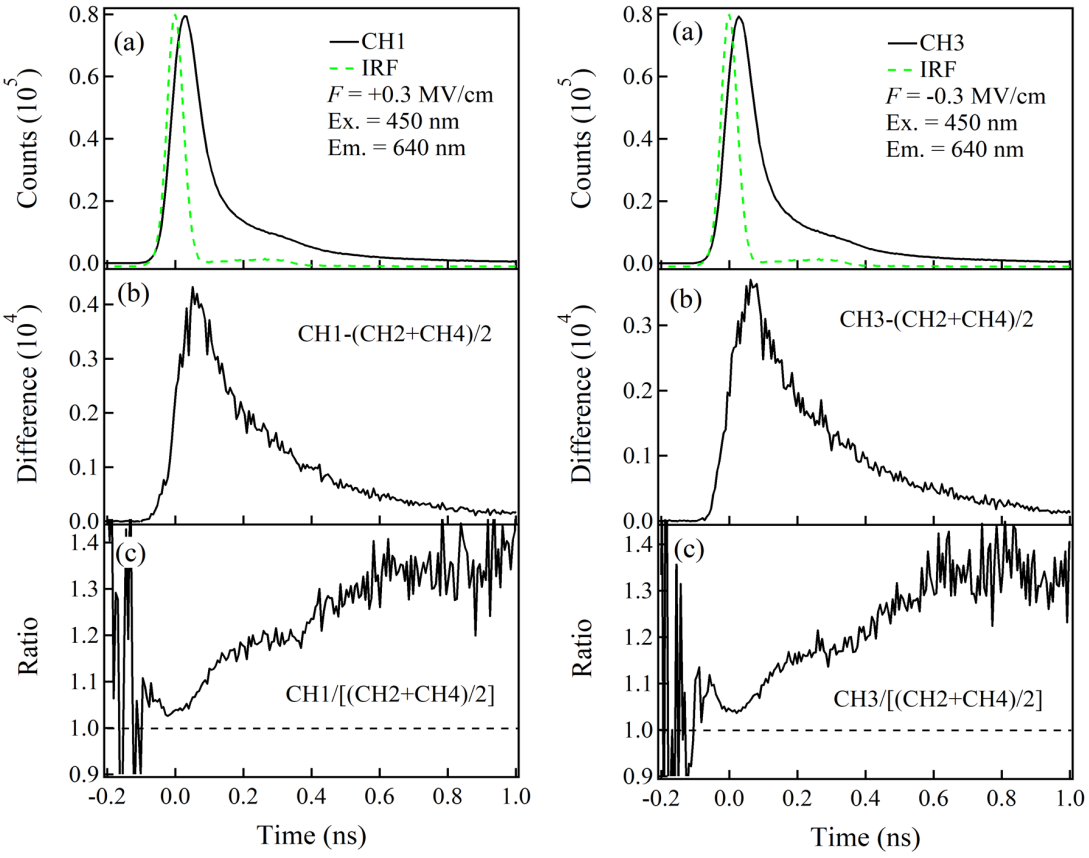

Figure 5. (a) PL decay profile observed at 640 nm in the presence of +0.3 $MVcm^{-1}$, i.e., CH1 (left) and -0.3 $MVcm^{-1}$, i.e., CH3 (right), (b) difference between CH1 and (CH2+CH4)/2 (left) and between CH3 and (CH2+CH4)/2 (right), and (c) ratio between CH1 and (CH2+CH4)/2 (left) and between CH3 and (CH2+CH4)/2 (right). Note that (CH2+CH4)/2 corresponds to the decay at zero field.

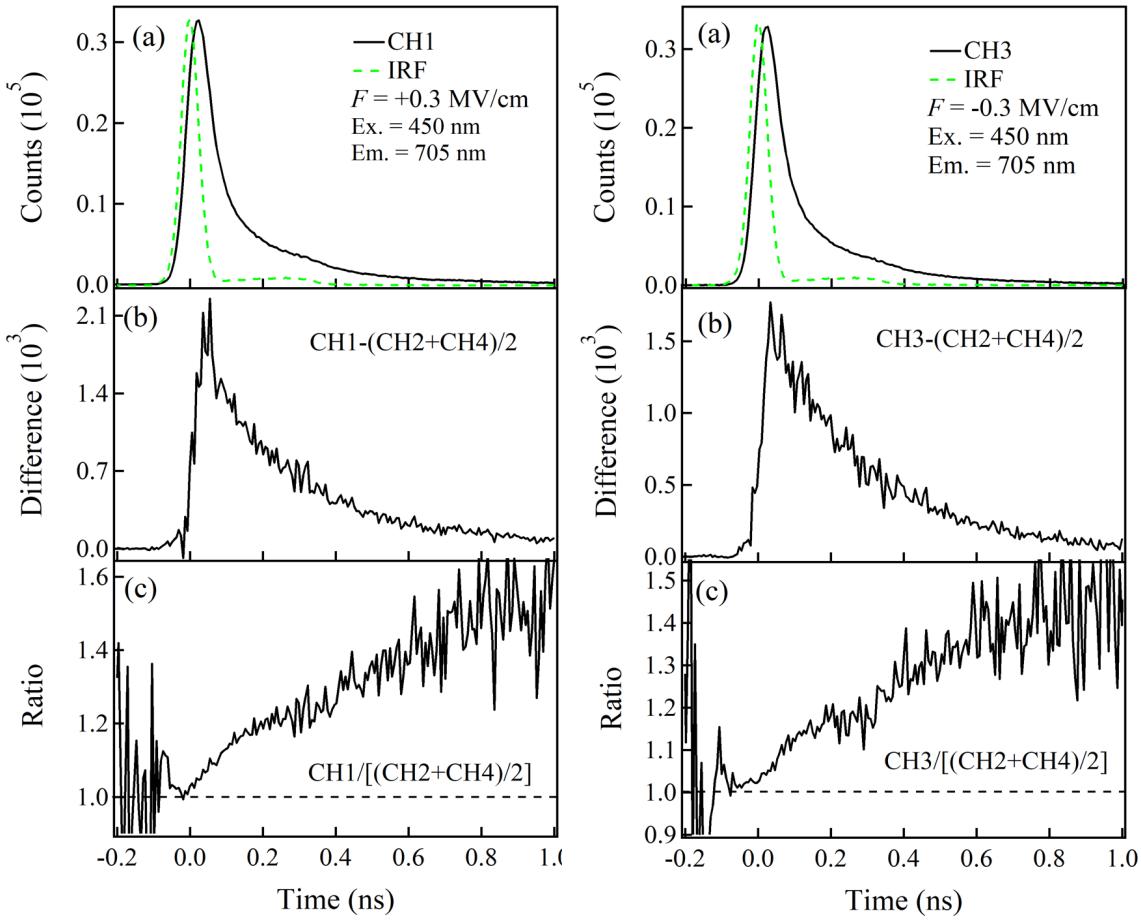

Figure 6. (a) PL decay profile observed at 705 nm in the presence of +0.3 $MVcm^{-1}$, i.e., CH1 (left) and -0.3 $MVcm^{-1}$, i.e., CH3 (right), (b) difference between CH1 and (CH2+CH4)/2 (left) and between CH3 and (CH2+CH4)/2 (right), and (c) ratio between CH1 and (CH2+CH4)/2 (left) and between CH3 and (CH2+CH4)/2 (right). Note that (CH2+CH4)/2 corresponds to the decay at zero field.

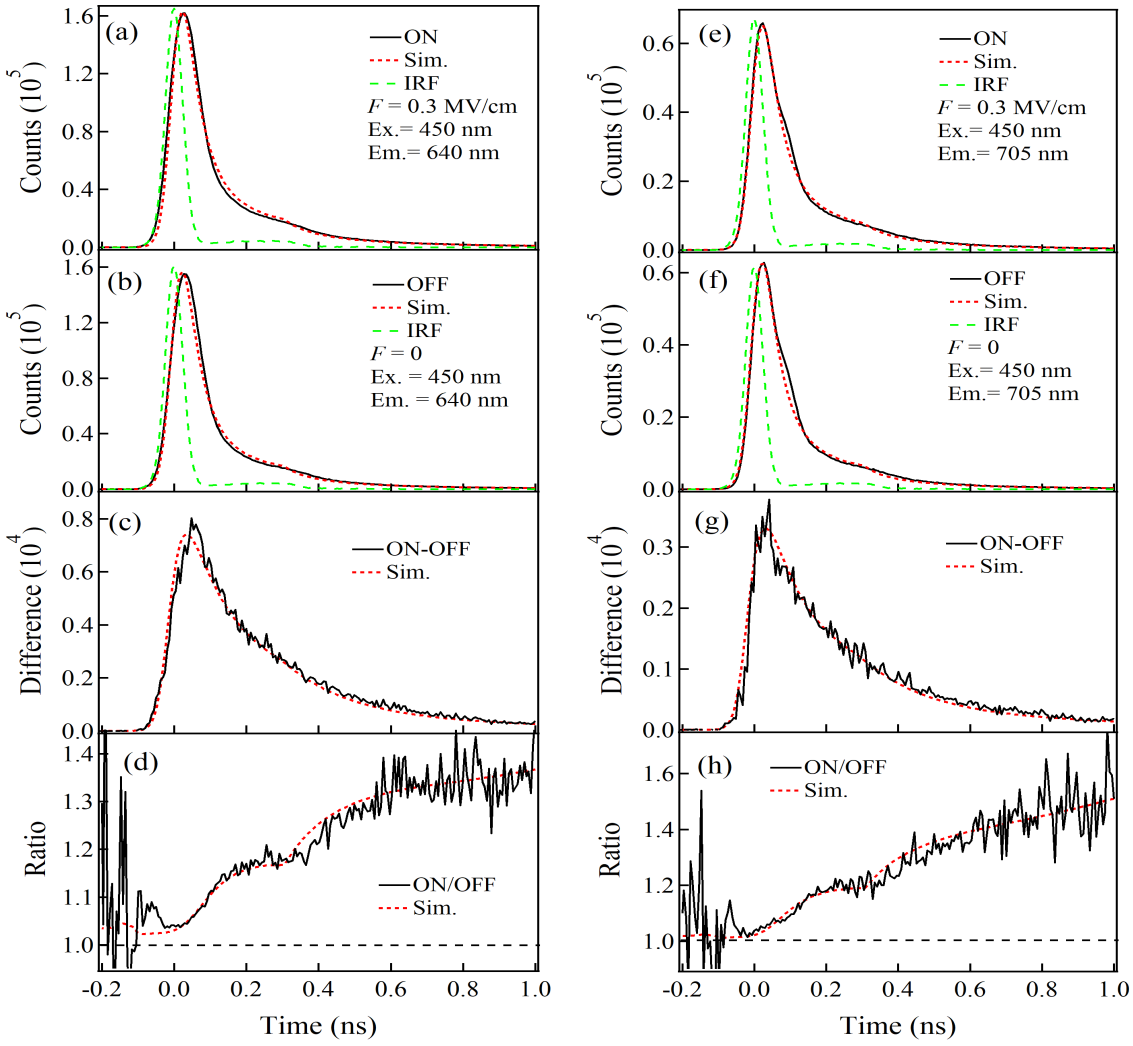

Fig. 7. PL decay profiles in the presence of 0.3 MVcm^{-1} and at zero field monitored at 640 nm (1.56×10^4 cm^{-1}) (left column) and at 705 nm (1.41×10^4 cm^{-1}) (right column) with excitation at 450 nm. (a,e) Decay profile of (CH1+CH3), i.e., $I(t)_{ON}$, (b,f) decay profile of (CH2+CH4), i.e., $I(t)_{OFF}$, (c,g) difference between $I(t)_{ON}$ and $I(t)_{OFF}$, and (d,h) ratio between $I(t)_{ON}$ and $I(t)_{OFF}$. Red line shows a simulation in every figure, and green line shown in (a,b,e,f) is the instrument response function (IRF).

TOC

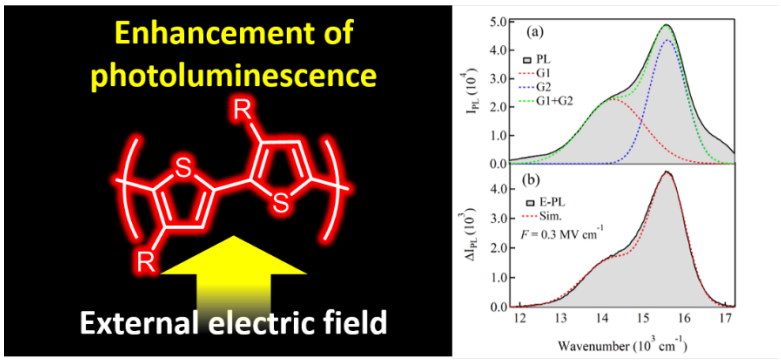

Enhancement of photoluminescence of P3HT dispersed in a PMMA film induced by application of electric field, as a quadratic field effect